Supporting information

Tumor-Acidity Activated Surface Charge Conversion of Two-Photon Fluorescent Nanoprobe for Enhanced Cellular Uptake and Targeted Imaging of Intracellular Hydrogen Peroxide

Lanlan Chen, *[abc] Shuai Xu,[c] Wei Li,[c] Tianbing Ren,[c] Lin Yuan,[c] Shusheng Zhang,*[a] Xiao-Bing Zhang*[c]

[a] *Collaborative Innovation Center of Tumor Marker Detection Technology, Equipment and Diagnosis-Therapy Integration in Universities of Shandong, Shandong Provincial Key Laboratory of Detection Technology for Tumor Markers, College of Chemistry and Chemical Engineering, Linyi University, Linyi, Shandong 276005, P. R. China*

[b] *The Key Lab of Analysis and Detection Technology for Food Safety of the MOE, Fujian Provincial Key Laboratory of Analysis and Detection Technology for Food Safety, College of Chemistry, Fuzhou University, Fuzhou 350002, P. R. China*

[c] *Molecular Science and Biomedicine Laboratory, College of Chemistry and Chemical Engineering and College of Biology, State Key Laboratory of Chemo/Biosensing and Chemometrics, Collaborative Innovation Center for Chemistry and Molecular Medicine, Hunan University, Changsha 410082.*

Experimental Section

Chemicals and reagents.

Glycol chitosan (M_w = 250,000, degree of deacetylation = 82.7%) was purchased from Sigma-Aldrich. 4-bromo-1, 8-naphthalic anhydride, bis(pinacolato)diboron, γ-aminobutyic acid, 1-ethyl-3-(3-(dimethylamino) propyl) carbodiimide hydrochloride (EDC) and *N*-hydroxysuccinimide (NHS) were purchased from Aladdin. All other reagents and solvents are of analytical grade and used without further purification.

Instruments and measurements.

^{1}H NMR spectra were recorded on a Bruker Advance (400 MHz) spectrometer with deuterated chloroform ($CDCl_3$), deuterated oxide (D_2O) and deuterated dimethyl sulfoxide (DMSO-d_6) as solvents. Fourier-transform infrared (FT-IR) spectra were performed on a Bruker TENSOR27 spectrometer in the range of 4000-400 cm^{-1} by pressing samples into pure potassium bromide pellets. Transmission electron microscopy (TEM) images were obtained with a JEOL JEM-2100F instrument operated at 200 kV. Dynamic light scattering (DLS) measurements were carried out on Malvern Zetasizer Nano ZS apparatus equipped with a 633 nm He-Ne laser. To determine the hydrodynamic diameter and study the stability of the nanoprobe, samples at different concentration in pH 7.4 PBS and 10% FBS were measured at a scattering angle of 90º at 25 ºC. For zeta-potential pH titrations, 10 mM HEPES buffer solution was prepared with pH values ranging from 6.00 to 7.8 in 0.2 unit increments. The sample was diluted to a final concentration of 200 μg/mL in the buffer at each pH, and zeta potential of the nanoprobe was measured using a Zetasizer Nano ZS. Each measurement was performed three times, and standard deviations were calculated as error bars. UV-Vis spectra were measured on a Shimadzu UV-2600 spectrometer. Fluorescence spectra were performed on a Hitachi F-4600 spectrofluorometer at room temperature. The fluorescence measurements were taken at an excitation wavelength of 450 nm, and the emission was monitored from 460 to 750 nm.

Synthesis of NABP (molecule 2)

Before synthesis of NABP, molecule 1 was synthesized. Briefly, a solution of 4-bromo-1,8-naphthalic anhydride (500 mg, 1.8 mmol) and bis(pinacolato)diboron (685 mg, 2.7

mmol) in anhydrous dioxane (10 mL) was stirred and refluxed under a N_2 atmosphere overnight. The solution was cooled to room temperature and extracted with CH_2Cl_2. The organic phase was washed with deionized water, dried with Na_2SO_4, concentrated and purified by silica gel column chromatography using hexane/CH_2Cl_2 (2:1, v/v) to afford 230 mg of **1** (40%).

A solution of **1** (200 mg, 0.62 mmol) and γ-aminobutyic acid (88.7 mg, 0.86 mmol) in anhydrous ethanol (5 mL) was stirred and refluxed for 4h under a N_2 atmosphere. After cooling to room temperature, the precipitate was separated by filtration, washed with ethanol and dried under vacuum at 40 ºC to give **2 (NABP)** (155 mg, 61%). ^{1}H NMR ($CDCl_3$, 400 MHz): δ 9.11(d, 1H), 8.59 (d, 1H), 8.55 (d, 1H) 8.29 (d, 1H), 7.77 (t, 1H), 4.26(t, 2H), 2.48 (t, 2H), 2.1 (m, 2H), 1.45 (s, 12H). ^{13}C NMR (DMSO, 100 MHz,) δ 174.41, 163.85, 163.83, 135.95, 134.86, 134.49, 130.75, 129.65, 127.83, 127.57, 124.77, 122.74, 84.91, 39.66, 31.83, 25.17, 23.44. HRMS *m*/*z* $[M + Na]^+$: 432.2

Synthesis of GC-NABP and Self-Assembled of the Nanoprobe.

To obtain GC-NABP, GC (93.35 mg, 0.40 mmol) was completely dissolved in 20 mL deionized water, and a DMSO solution (5 mL) containing NABP (40.90 mg, 0.10 mmol), EDC (23.00 mg, 0.12 mmol) and NHS (13.81 mg, 0.12 mmol) was added. The reaction mixture was stirred at ambient temperature for 24 h, and the resulting solution was purified by dialysis against 1:4 (*v*/*v*) DMSO/H_2O for 1 day. GC-NABP was self-assembled into nanosized micelle by further dialysis against deionized water for another 1 day (MWCO: 14 kDa). The resulting dispersions of nanoparticles were lyophilized or used as is for characterization. The dried GC-NABP nanoprobe could be redispersed in water at 1 mg mL^{-1} under sonication for several minutes for further use.

Labelling GC-NABP with Cy5.5 and preparation of control nanoparticles GC-OH-NABP-Cy5.5. Cy5.5-labelled GC-NABP (GC-NH_2-NABP-Cy5.5) was synthesized as follow. Briefly, a solution of Cy5.5-NHS in DMSO was added in GC-NABP solution (10 mM PBS, pH 8.5). The weight ratio of Cy5.5 to GC-NABP was 1:100 (w/w). The solution was stirred at room temperature in the dark for 12 h. Byproducts and unreacted Cy5.5 were removed by dialysis against deionized water with 150 mM NaCl and then against deionized water (MWCO: 14 kDa). The resulting

products were lyophilized for further use.

Control nanoparticles GC-OH-NABP-Cy5.5 were prepared by directly chemical modification of GC-NABP-Cy5.5 nanoparticle surface. 3 mL glycidol was added in 1.5 mL GC-NABP-Cy5.5 solution (1 mg/mL, 10 mM PBS) and the mixture was incubated at room temperature in the dark for 24 h. Excess glycidol was removed by dialysis against deionized water with 150 mM NaCl and then against deionized water (MWCO: 14 kDa). The resulting products were lyophilized for further use.

Measurement of Two-Photon Absorption Cross Section. The two-photon cross section was measured by femtosecond fluorescence analysis system. Samples (10 μM) were dissolved in PBS buffer (10 mM, pH 7.4,). Rhodamine B was used as reference to measure the intensities of two-photon excited fluorescence at 720-840 nm. The two-photon absorption cross section was calculated with $\delta = \delta_r(F_s n_s^2 \Phi_r c_r)/(F_r n_r^2 \Phi_s c_s)$[1], where the s and the r subscript stand for sample and reference molecules, respectively. F is the average fluorescence intensity, n is the refractive index of the solvent, Φ is the quantum yield, c is the concentration, and δ_r is the two-photon cross section of the reference[2].

Cells Culture and *In Vitro* Cytotoxicity Assay. Hela cells and HepG2 cells were cultured in Dulbecco's Modified Eagle Medium (DMEM) supplemented with 10% fetal bovine serum (FBS), penicillin (100 units/mL) and streptomycin (100 μg/mL) at 37 ºC under a CO_2/air (5:95) humidified atmosphere. For cytotoxicity assay, Hela cells were seeded in a 96-well plate at an initial density of 5000 cells/well in 120 μL of complete DMEM medium. After incubating at 37 ºC for 24 h, DMEM was replaced with fresh medium, cells were treated with GC-NABP nanoprobe at different concentrations and incubated at 37 ºC for another 24 h. Then 20 μL of MTT (methyl tiazolytetrazolium, 5 mg/mL in PBS) was added to each well. After incubating for another 4 h, the medium was removed and replaced by 100 μL DMSO to dissolve blue formazan crystals, followed by gently shaking for 15 min. The absorbance at 490 nm was recorded by a microplate reader (Bio-Tek).

Flow Cytometry. Hela cells were seeded in six-well plate (5.0×10^4 cells/well) and

cultured for 24 h. The medium was replaced with fresh medium of pH 7.4 or 6.5 containing 200 μg/mL GC-NABP nanoprobe. After incubation for 4 h at 37 ºC, the cells were washed thrice with DPBS and treated with 200 μM H_2O_2 for another 1 h. After removing the medium and subsequently washing with DPBS, the cells were trypsinized, centrifuged and resuspended in 0.5 mL DPBS. The fluorescence signals of cells labeled with the nanoprobe were analyzed by flow cytometry (Beckman, CytoFlex). 20,000 cells were recorded and data were analyzed using FlowJo software.

Fluorescence Imaging of Hydrogen Peroxide in Living Cells by Confocal Laser Scanning Microscopy (CLSM). To investigate H_2O_2 imaging performance of the GC-NABP nanoprobe at different pH values, HepG2 cells were seeded in dishes at a density of 1.0×10^4 and incubated in 2 mL culture medium (pH 7.4) at 37 ºC for 24 h. Subsequently, the medium was replaced with fresh medium of pH 7.4 or 6.5, and then the GC-NABP nanoprobe was added at a concentration of 200 μg/mL. After incubation for 4 h, cells were washed with DPBS thrice and incubated with fresh medium containing 200 μM H_2O_2 for another 1 h. In cases of LPS simulation, cells were pretreated with 1 μg/mL LPS for 12 h and washed by DPBS. Then fresh medium of pH 7.4 or 6.5 containing the nanoprobe were added. After incubation for 4 h, the medium was replaced by DPBS for imaging experiments. Cells in DPBS were observed by CLMS (Nikon, Ti-E + A1 R MP) with $\times$40 water objective lens and collection wavelength range of 500-550 nm excited at 780 and 488 nm for two-photon microscopy (TPM) and one-photon microscopy (OPM) images, respectively. Pixel fluorescence intensity of CLMS images were analyzed by Image-Pro Plus software. Each analysis was carried out three times, and standard deviations were calculated as error bars.

Subcellular localization of the GC-NABP nanoprobe. HepG2 cells were seeded in dishes at a density of 1.0×10^4 and incubated in 2 mL culture medium (pH 7.4) at 37 ºC for 24 h. Subsequently, the medium was replaced with fresh medium of pH 6.5, and then the GC-NABP nanoprobe was added at a concentration of 200 μg/mL. After incubation for 4 h at 37 and 4 ºC, cells were washed with DPBS thrice and incubated

with fresh medium containing 200 μM H_2O_2 for another 1 h. After removing the medium and subsequently washing wish DPBS thrice, the endosomes were stained with 1 μM lyso-tracker red for 10 min. Then the cells were washed by DPBS before imaging by CLSM.

Fluorescence Imaging of Hydrogen Peroxide in Tumor Tissues. Tissue slices were prepared from rat 4T1 tumor tissue. The slices were cultured with medium of pH 7.4 or 6.5 containing 200 μg/mL GC-NABP in an incubator at 37 ºC for 4 h and washed with DPBS thrice. Then, the slices were kept in culture medium with 200 μM H_2O_2 for another 1 h and washed with DPBS for TPM imaging. The measurements of tissue penetration depth were performed using Z-axis scanning mode. TPM images were collected with $\times$10 dry objective lens in wavelength range of 500-550 nm upon excitation at 780 nm.

Blood clearance measurement. All living mice studies were performed in accordance with animal care guidelines. Animal protocol (No. SYXK (Xiang) 2008-0001) was approved by the Laboratory Animal Center of Hunan. Healthy female BALB/c mice were purchased from Hunan SJA Laboratory Animal Co., Ltd. (Changsha, China) Healthy female BALB/c mice (~20 g, n=3) were used and given an intravenous injection of 200 μL, 1 mg/mL GC-NABP-Cy5.5 nanoprobe in PBS buffer. At timed intervals, 5 μL blood samples were diluted into 200 μL PBS before fluorescence intensity measurements.

Biodistribution measurement. 4T1 tumor-bearing female BALB/c mice were randomly divided into two group (n=3) and given an intravenous injection of GC-NABP-Cy5.5 or GC-OH-NABP-Cy5.5 at 1 mg/mL in 200 μL PBS buffer. After 24 h after the injection, main organs and tumors were harvested and imaged using Lumina XR In-Vivo imaging system (PekinElmer Inc.).

Tumor-targeting Imaging of Hydrogen Peroxide in tumor-bearing mice model. The tumor model was constructed by subcutaneous injection with 100 μL 4T1 cells

suspension (a density of 2×10^6 cells/mL in DPBS) into the right flank of mice. When the volume of the tumor xenograft reached 60~70 mm^3, the mice were given an intravenous injection of 100 μL, 1 mg/mL GC-NABP nanoprobe in DPBS. Twenty-four hours after the injection, the mice were sacrificed and tumor tissues were harvested and imaged using two-photon confocal microscopy.

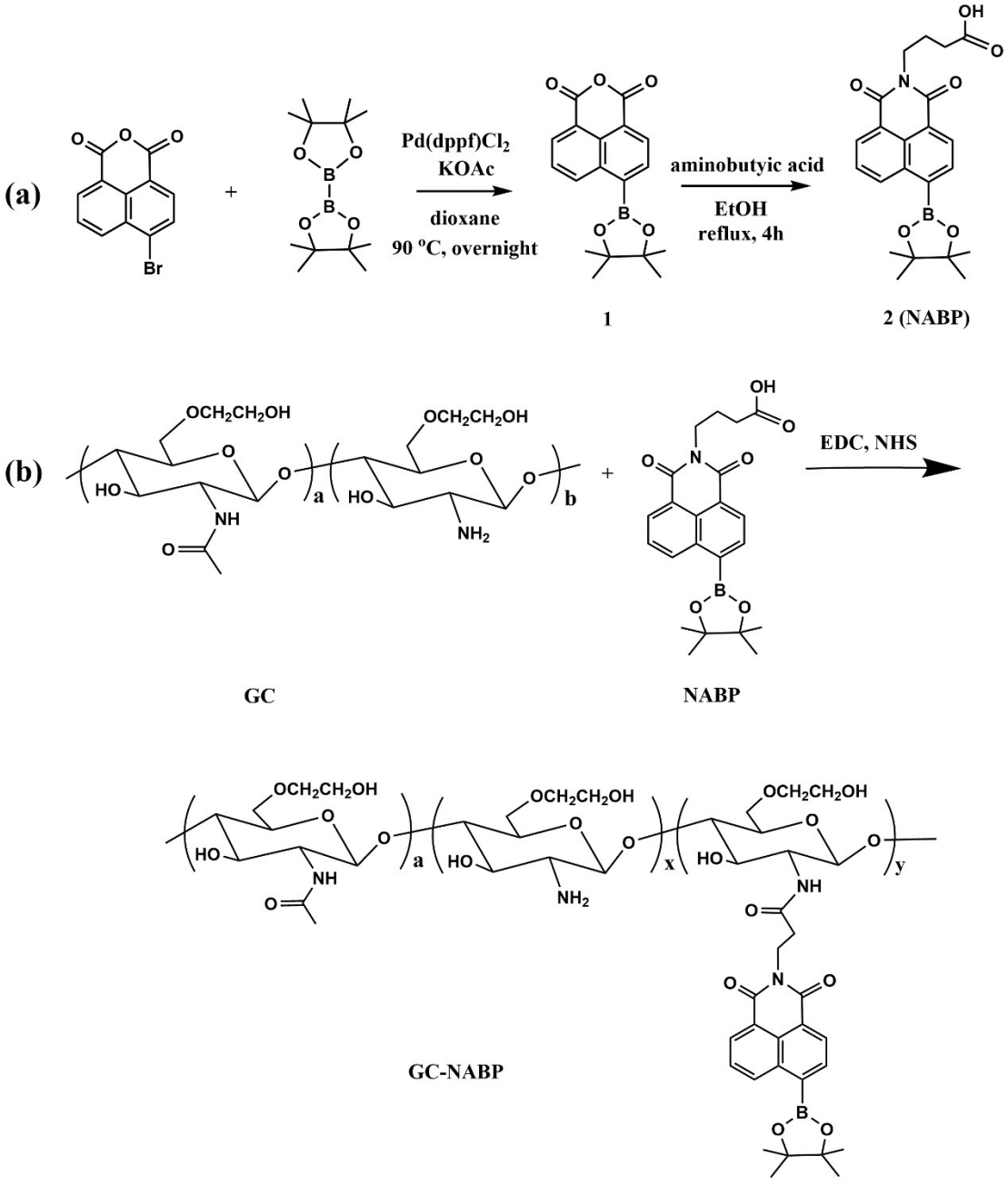

Fig. S1 Synthesis of **1**, **2 (NABP)** and **GC-NABP**.

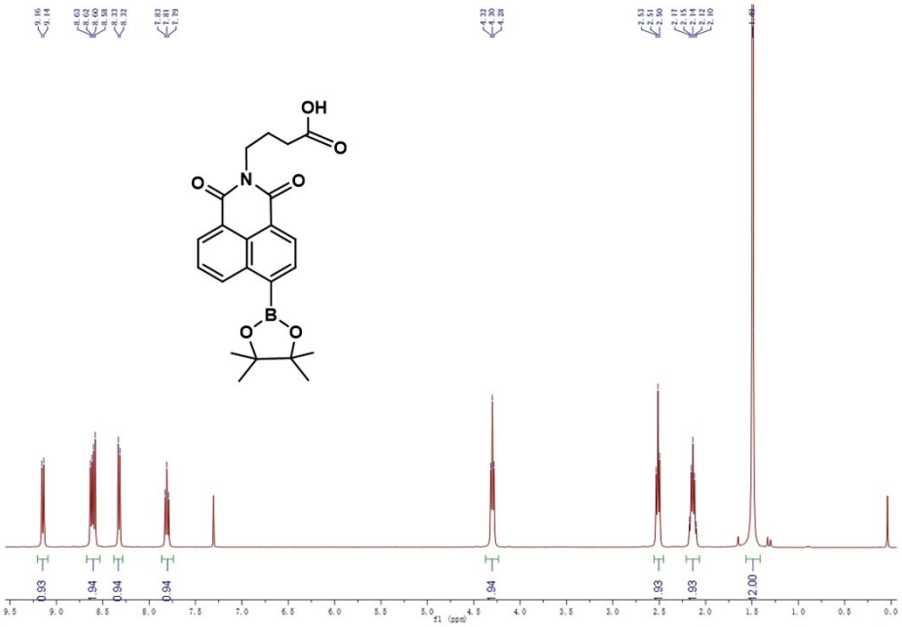

Fig. S2 ^{1}H NMR spectrum of **2 (NABP)**.

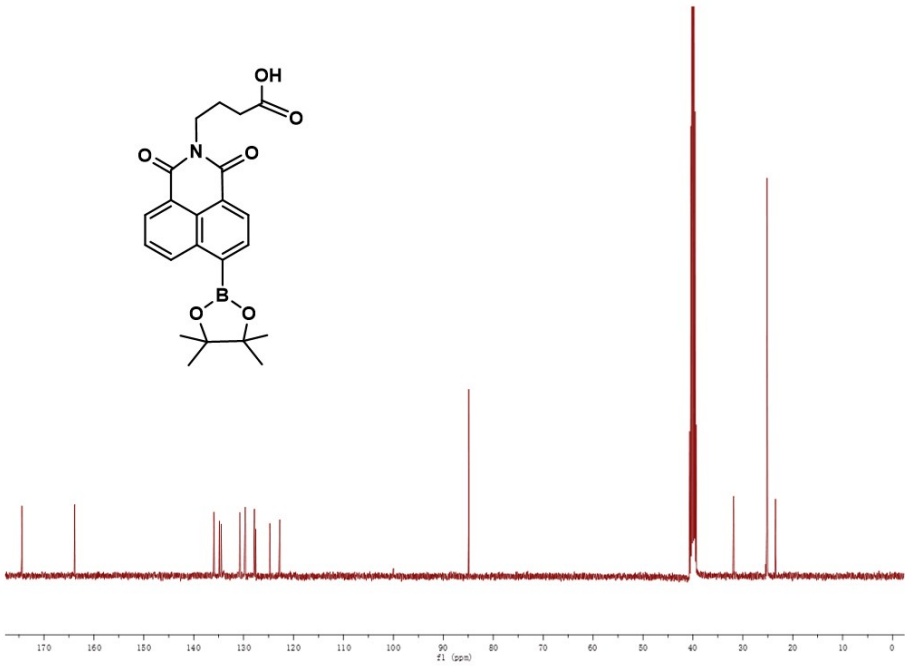

Fig. S3 ^{13}C NMR spectrum of **2 (NABP)**.

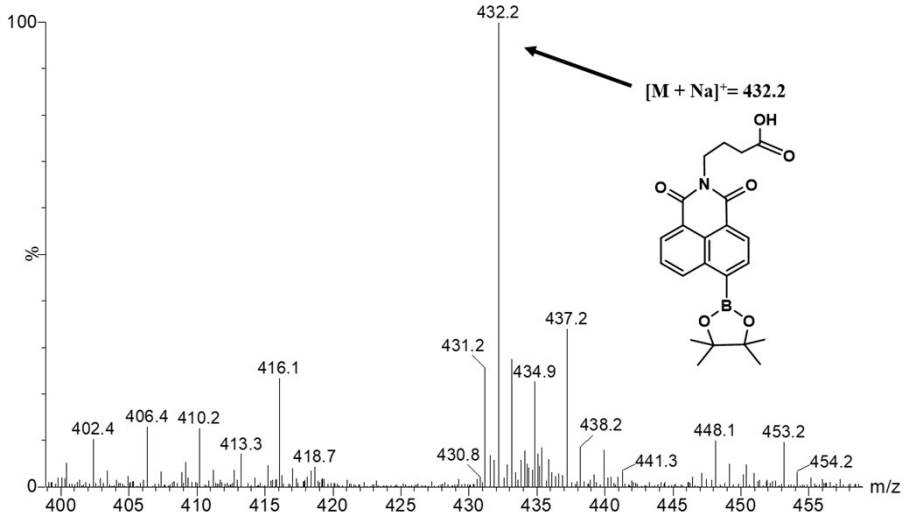

Fig. S4 HRMS spectrum of **2 (NABP)**

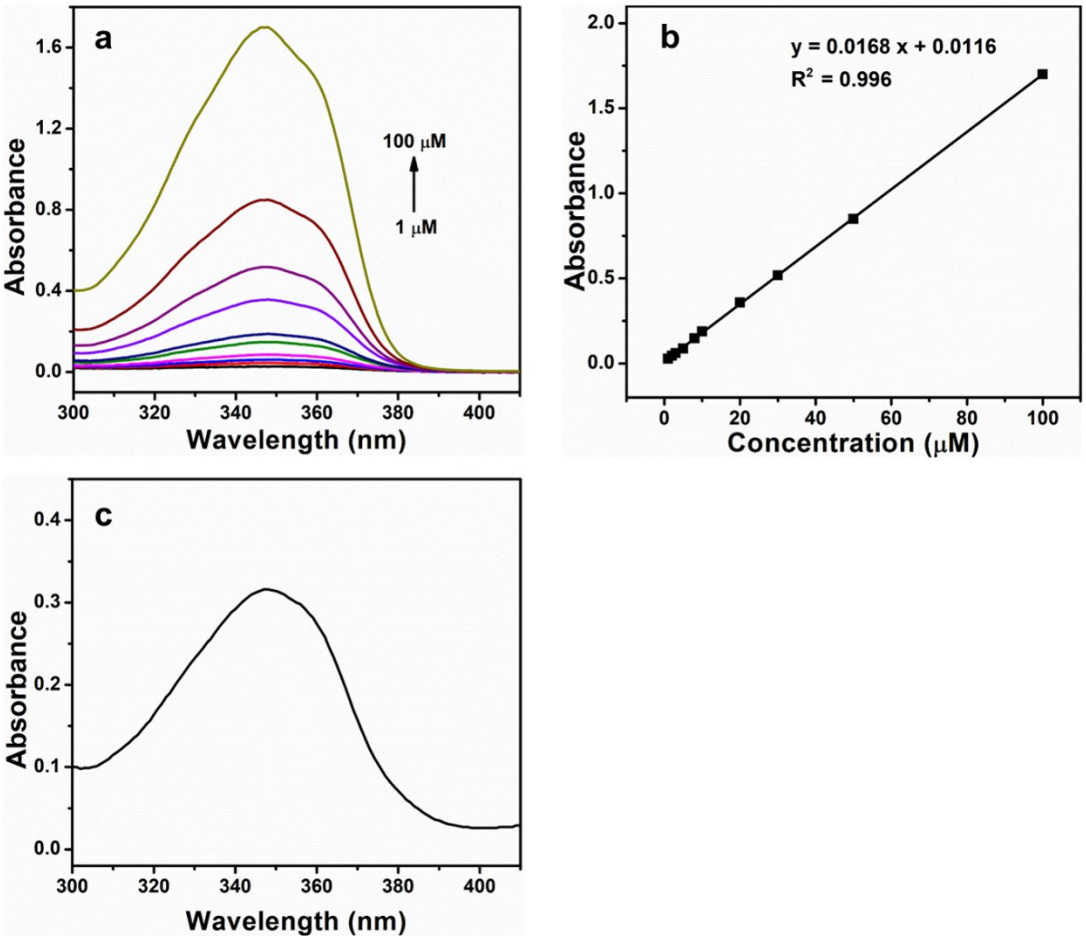

Fig. S5 (a) UV-Vis spectra of NABP in DMSO at concentration range from 1 to 100 μM. (b) Dependence of absorbance at 350 nm on concentration of NABP. (c) UV-Vis spectrum of GC-NABP (20 μg/mL).

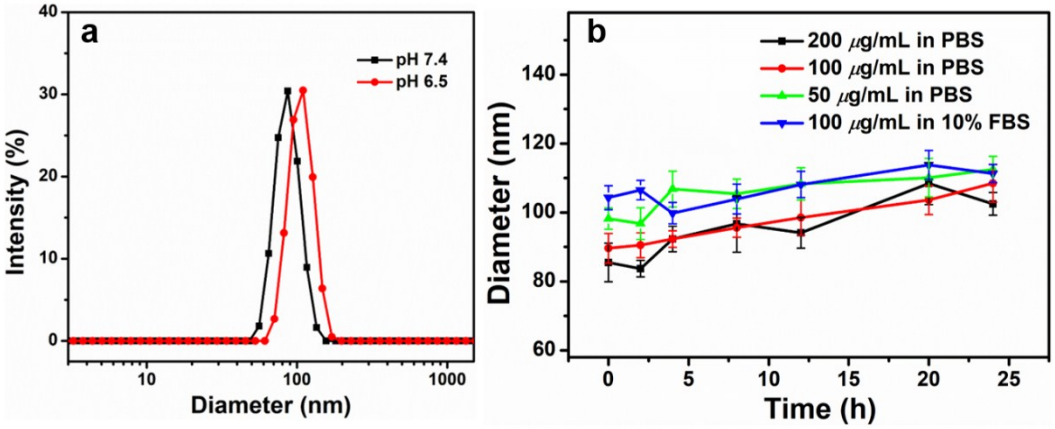

Fig. S6 (a) DLS measurements of GC-NABP nanoprobe (200 μg/mL) in pH 7.4 and 6.5 PBS.(b) Size change of GC-NABP nanoprobe at different concentration in pH 7.4 PBS (50, 100, 200 μg/mL) and in 10% FBS (100 μg/mL) in 24 h determined by DLS.

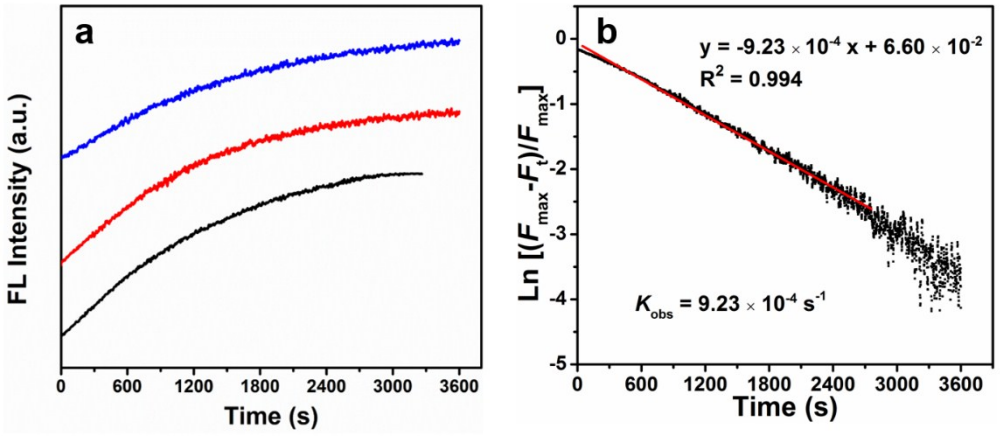

c

Experiment #	y = ax + b	R^2	K_{obs} (s^{-1})
1	$y = -8.82 \times 10^{-4} x + 4.99 \times 10^{-2}$	0.997	8.82×10^{-4}
2	$y = -9.23 \times 10^{-4} x + 6.60 \times 10^{-2}$	0.994	9.23×10^{-4}
3	$y = -6.58 \times 10^{-4} x + 3.74 \times 10^{-1}$	0.995	6.58×10^{-4}
Average K_{obs}			$8.21 \pm 1.43 \times 10^{-4}$

Fig. S7 (a) Time-dependent evolution of normalized fluorescent intensity at 550 nm recorded for GC-NABP nanoprobe incubated with 10 mM H_2O_2. (b) The pseudo first-order kinetic plot of the reaction of GC-NABP nanoprobe with a large excess of H_2O_2 (red line in (a)). (c) fitted data of the pseudo first-order kinetic.

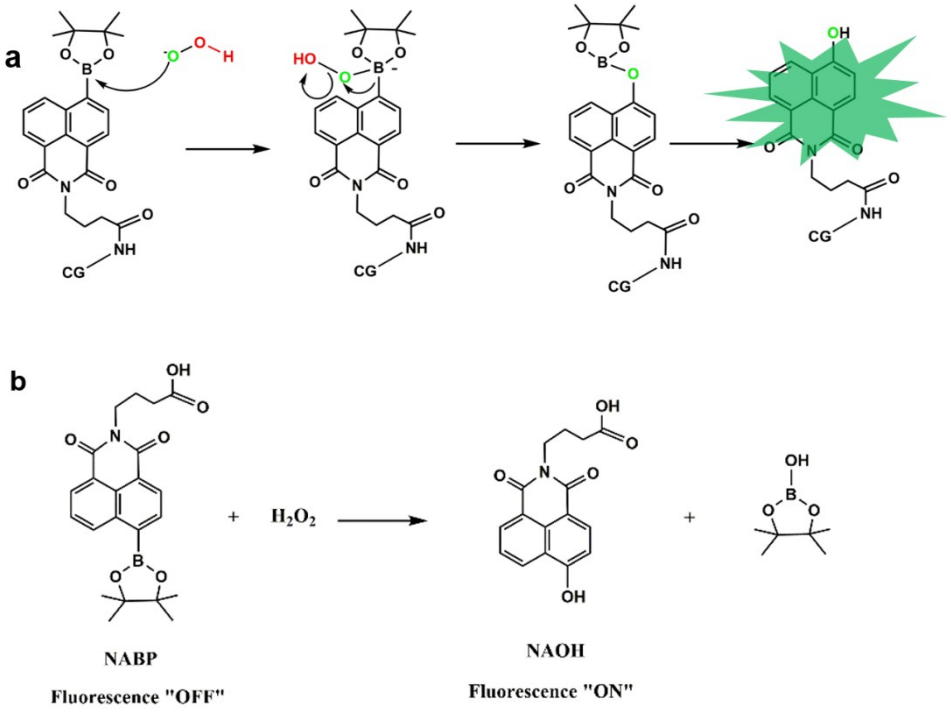

Fig. S8 (a) Mechanism of GC-NABP nanoprobe for selective H_2O_2 detection. (b) Oxidation of NABP with H_2O_2

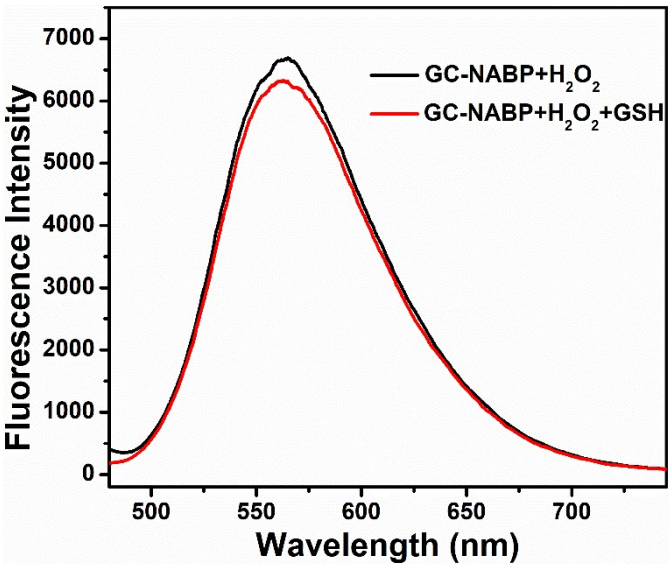

Fig. S9 Fluorescence spectra of GC-NABP nanoprobe treated with 200 μM H_2O_2 and then with and without incubation with GSH.

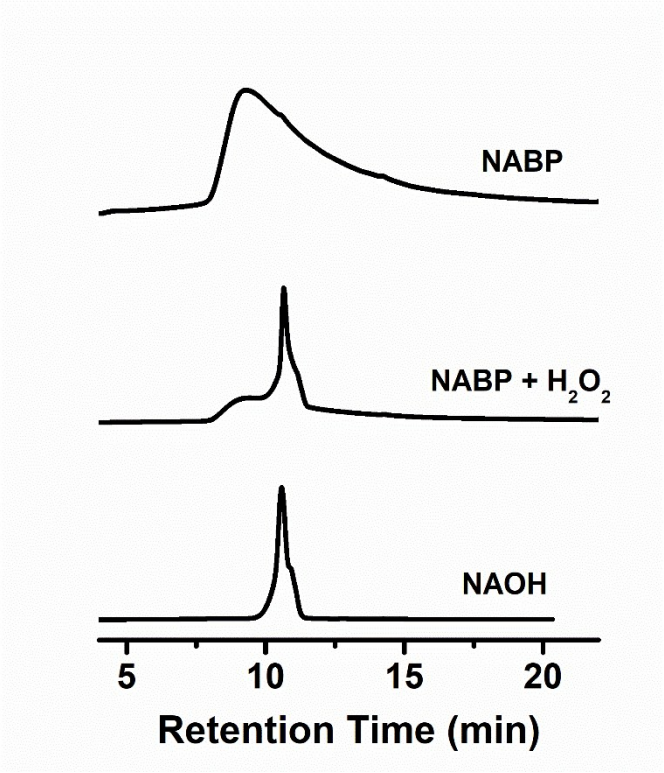

Fig. S10 HPLC traces of NABP, reaction mixture of NABP with H_2O_2, and NAOH.

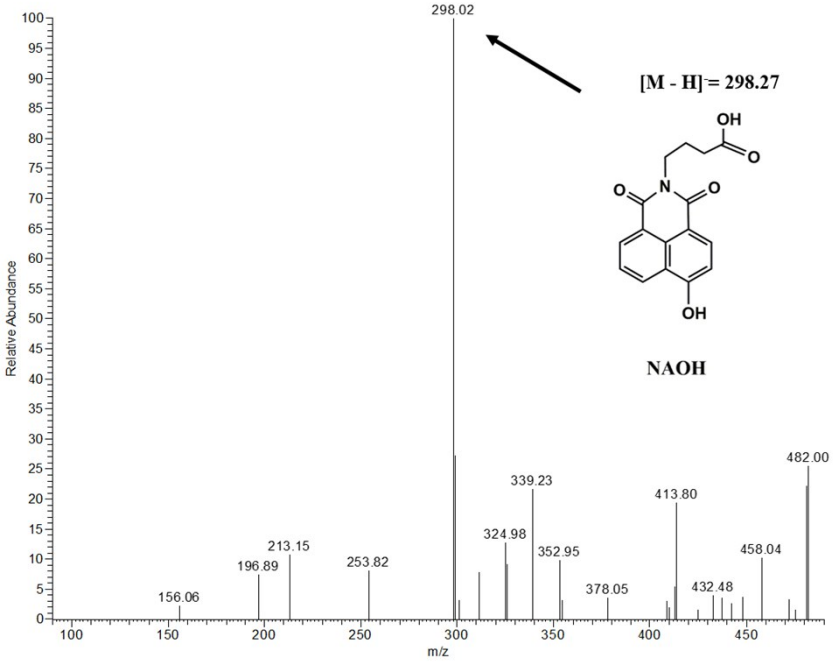

Fig. S11 ESI-MS spectra of NABP treated with H_2O_2.

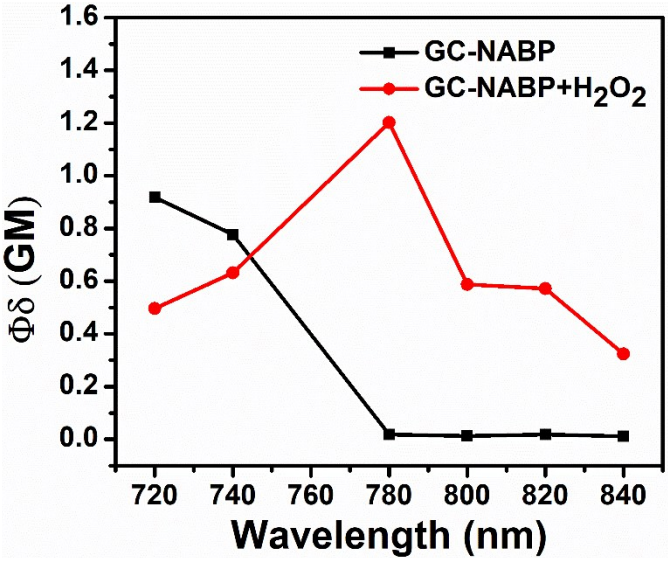

Fig. S12 Two-photon absorption cross section of GC-NABP in the absence and presence of H_2O_2 in PBS (10 mM, pH 7.4).

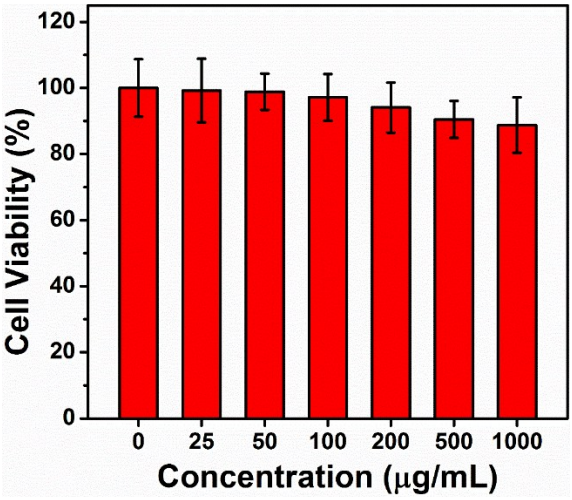

Fig. S13 Cytotoxicity of GC-NABP nanoprobe.

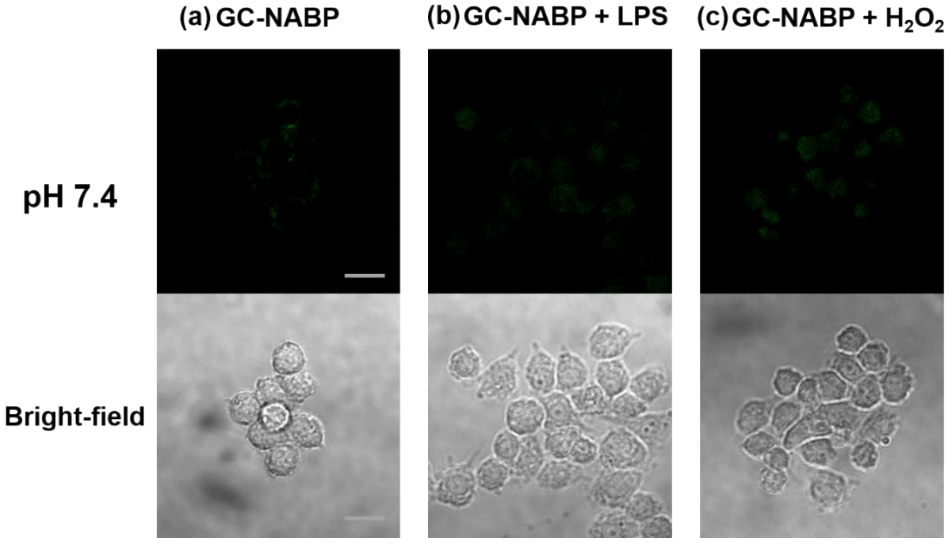

Fig. S14 Two-photon microscopy image and bright-field images of RAW264.7 cells incubated with only GC-NABP nanoprobe (a), simulated with LPS and then treated with GC-NABP nanoprobe (b) and treated with GC-NABP nanoprobe and H_2O_2 (c) at pH 7.4. Scale bar: 20 μm.

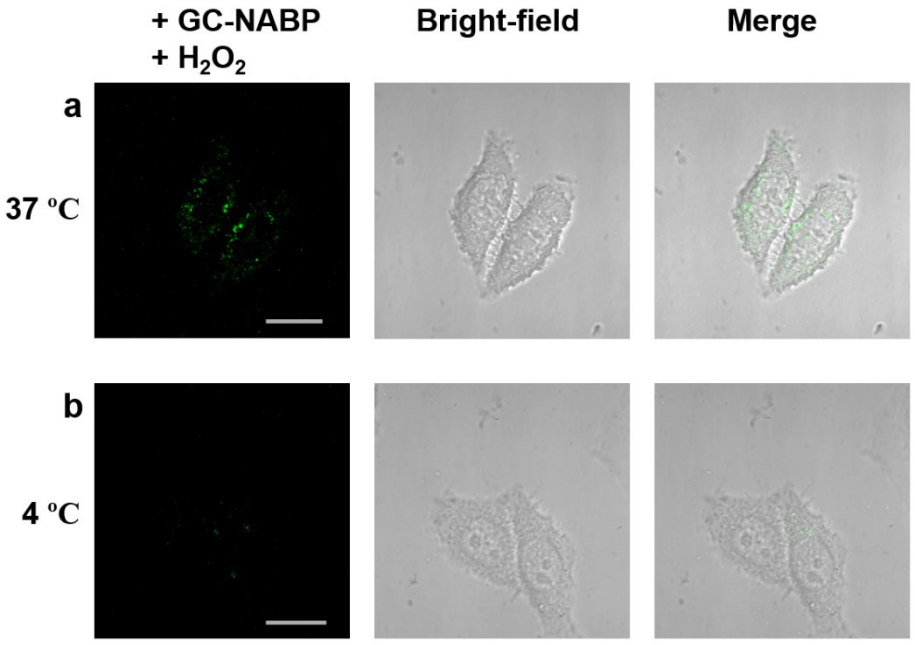

Fig. S15 CLSM images of HepG2 cells were incubated with GC-NABP nanoprobes at 37 °C (a) and 4 °C (b) for 4 h, and then with 200 μM H_2O_2 for another 1 h. Scale bar = 20 μm.

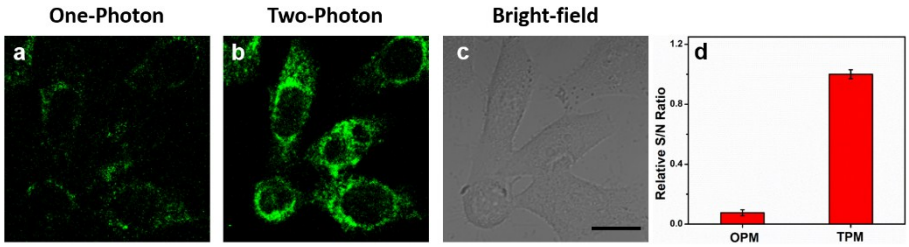

Fig. S16 OPM image (a), TPM image (b) and bright-field image (c) of HepG2 incubated with the GC-NABP nanoprobe and H_2O_2 at pH 6.5. (d) Relative signal-to-noise ratio of OPM and TPM. Scale bar: 20 μm.

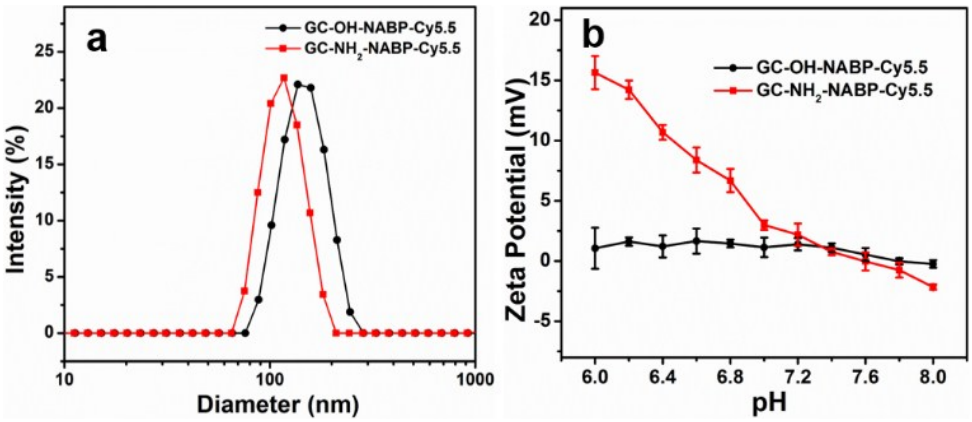

Fig. 17 (a) DLS measurements of GC-OH-NABP-Cy5.5 (200 μg/mL) and GC-NH_2-NABP-Cy5.5 (200 μg/mL). (b) Zeta potential of GC-OH-NABP-Cy5.5 and GC-NH_2-NABP-Cy5.5 in buffers at different pH.

References

1 Ren, T.; Xu, W.; Jin, F.; Cheng, D.; Zhang, L.; Yuan, L.; Zhang, X. B. *Anal. Chem.* **2017,** *89*, 11427-11434.

2 Makarov N. S.; Drobizhev M.; Rebane A. *Opt. Exp.* **2008,** *16*, 4029-4047.